ROUTINE COMPARISON OF OBSERVED AND MODELLED CLOUDS

L. Rikus and J. Kepert
Australian Bureau of Meteorology Research Centre
Melbourne,Vic.,Australia 3001

Abstract: The BMRC cloud validation scheme is a simple scheme based on geostationary satellite infrared data which has been used to assess the performance of the diagnostic cloud parameterization scheme in the Australian Bureau of Meteorology's operational medium range forecast model since November 1991.This paper describes the scheme and reviews some of the monthly averaged cloud fields during that period.

1. INTRODUCTION

The question of how best to represent cloud and its interaction with radiation is an important issue in numerical weather prediction (NWP). It is well known that the simulations of climate change in general circulation models (GCM's) are very sensitive to their cloud/radiation parameterization schemes (Cess et al 1990). Although the cloud schemes are generically the same in NWP models the context changes the requirements of the parameterization ; in this case it is required to accurately reproduce the structure and changes in a real-time cloud field (or at least the radiative properties of cloud) over short time scales of a few hours to a few days. NWP cloud schemes must also cope with errors in the initial conditions due to insufficient data to characterise the water vapour field and the spin up of the model hydrology due to thermodynamic imbalances in the initial state.

Cloud/radiation effects are important for medium range forecasts, not only because of the interaction with the convection scheme which can determine certain aspects of the hydrological cycle in the first few days of the forecast, but also because longer range forecasts become increasingly sensitive to the details of the parameterization. When the model is an integral component of an assimilation system the details of the cloud/radiation parameterization have a strong influence on the basic 'climate' state of the model, particularly in regions of sparse data and for fields such as water vapour, that are not well represented by model parameterization schemes or not well characterised by data from the observational network. Hence the behaviour of the cloud/radiation scheme in an NWP model has a fundamental influence on the performance of a medium range prediction model.

There are other reasons for looking at a model's representation of cloud fields. Forecasts of cloud amount and height are clearly of interest to operational meteorologists and many of their clients, not only as a

visualisation tool for large scale weather system behaviour but also as a product in its own right. Such forecasts may be useful as input to satellite data acquisition schemes that require prior knowledge of cloud amount and placement. Those modellers responsible for maintenance of the operational model should also be interested in forecast cloud because by its very nature it provides an excellent tracer of the model's simulation of the global hydrological cycle.

Clearly for all the above reasons the behaviour of an operational model's cloud/radiation scheme needs to be assessed on a regular and timely basis. A real-time validation scheme has a number of advantages over a scheme which considers only a limited number of historical case studies, even if the latter may allow the use of more extensive datasets which are not available in real-time. Provided the validation scheme is incorporated as part of the operational cycle any extra data storage space and computer processing time are minimised because all the resources are already in place. Over time the cloud validation scheme samples all common ranges of meteorological and current climate situations. By construction the version of the model is consistent with the ongoing assimilation, minimising spin up effects. In an operational context problems in the model become apparent as they occur. Finally, because it provides a link between real and modelled cloud, a real-time cloud validation scheme can be used as a source of continuous correction in a statistical parameterization scheme (Rikus and Hart 1988, Mitchell and Hahn 1990).

This paper describes a real-time cloud/radiation validation scheme which has been in operation at the Australian Bureau of Meteorology since November 1991. The operational NWP model upon which it is based is described in the next section. This is followed by a description of the validation scheme itself and a discussion of some results from the scheme.

2. THE BMRC GLOBAL SPECTRAL MODEL

2.1 **Model evolution**

The operational NWP model form of the BMRC Global Atmospheric Model (GAM) is used for medium range forecasts and to supply boundary conditions for shorter range regional forecast models. When the cloud validation scheme was first implemented in November 1991, the model used 9 sigma levels in the vertical but this changed to 19 levels in December 1992, in conjunction with modifications to some of the physical parameterization schemes and the introduction of an MVSI assimilation scheme. The spectral resolution was initially rhomboidal 31 but changed to rhomboidal 53 in late March 1994. The operational assimilation cycle is run twice a day, each time to assimilate 12 hours of data, with analyses archived every 6 model hours. Global forecasts are made from the 23Z and 11Z analyses with the results saved

for every 24 hours of model time.

The basic physical parameterizations for the 9 level model have been described in detail elsewhere (Hart et al, 1990). The modelling of radiative transfer is based on the Fels and Schwarzkopf (1975) (Schwarzkopf and Fels, 1991) parameterization scheme in the longwave and Lacis and Hansen (1974) in the shortwave. The main change affecting the model's hydrology over the period to be considered here, was to the specification of the moistening parameter (usually referred to as the b parameter) in the Kuo scheme (Kuo 1974, Anthes 1977). Initially in the R31L9 model the 'b' parameter was assumed to be the standard cubic function of relative humidity ranging over values from 1 to 0 for relative humidity running from 0 to 100%. For the 19 level models the 'b' parameter is a cubic for values of relative humidity over 50%, and set to 1 otherwise. This results in a moister troposphere and less convective heating (Tada et al, 1989). Another relevant change was in the assimilation of water vapour. Moisture was assimilated up to the 0.336 sigma level in the 9 level model, but only up to the 0.400 sigma level in the 19 level model. During the period of operation of the 9 level model the sea surface temperatures (SST's) were input from a climatological data set (Alexander and Mobley 1976) and were kept constant for each month. The 19 level model used SST's updated weekly from a real-time data set (Reynolds and Marisco 1993).

2.2 The model diagnostic cloud scheme

In the diagnostic cloud scheme (Rikus 1991), cloud is partitioned into three height classes. The maximum relative humidity $RH_{max}(L)$ in each layer L is used to calculate a cloud amount $C(L)$ for that layer via,

$$C(L) = Max[\frac{(RH_{\max}(L) - RH_{crit}(L))}{(100 - RH_{crit}(L))}, 0]^2 \qquad (1)$$

The critical relative humidities are a function of sigma level and are given by an equation given by Geleyn (1981) for low and middle cloud. To ensure adequate cloud amounts in the tropics the critical value for high cloud has been set to 40%. Additional low cloud, corresponding to stratocumulus which is subgrid scale in the vertical (Slingo 1987) is diagnosed at the second bottom level of the model, according to,

$$C_{ST}(N-1) = MIN[-33.33(\Gamma - 0.03), 1.0] \qquad (2)$$

where N is the number of model sigma levels (numbered from the top of the model), and,

$$\Gamma = \frac{T(N-2) - T(N-1)}{p(N-2) - p(N-1)} \tag{3}$$

i.e. the vertical temperature gradient across the pressure layer above the bottom sigma level. $C_{ST}(N\text{-}1)$ is set to zero unless the relative humidity of the bottom level is greater than 60%. These parameters were chosen as those that gave the best representation of oceanic stratus in the regions southwest of Australia for a particular analysis in comparison with an infrared GMS-3 image for the 9 level model. The cloud in each layer is restricted to at most one level in each layer except in the low cloud layer where cloud can span two levels if there are two levels of high relative humidity or if the stratocumulus and relative humidity cloud amounts are comparable. The sigma level limits for cloud layers are shown in Fig. 1. On the changeover to 19 levels the cloud amounts for the layer limits denoted as 'original' were found to be excessive with a preference for cloud (particularly middle level cloud) to be diagnosed at the bottom of the layer (Rikus and Kepert, 1995). To alleviate this problem a modified scheme ('thin cloud'), in which the cloud was restricted to occur only at the levels closest to the original 9 levels (see Fig. 1), was introduced in mid-January 1993. In their interaction with radiation the clouds are assumed to be black body radiators in the longwave and have prescribed albedoes and absorptivities in the shortwave.

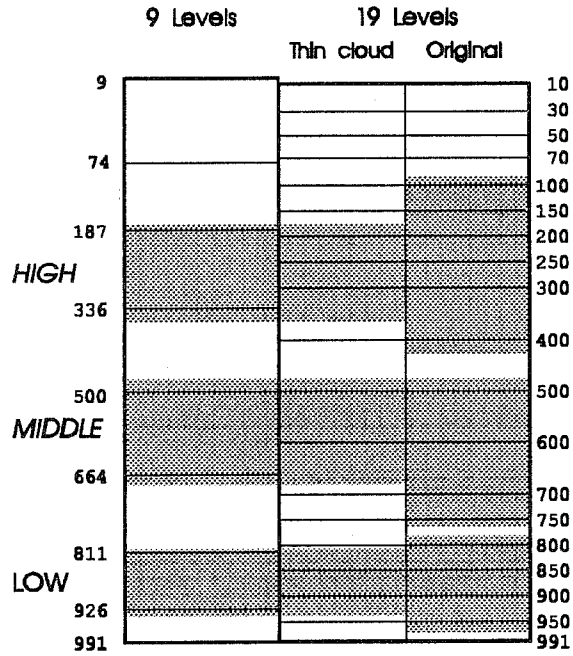

Figure 1 The sigma level structure (sigma * 1000) for the 9 level model (left) and the 19 level model (right). The shading indicates the layers in which relative humidity cloud was diagnosed for the different versions of the model.

3. VALIDATING BRIGHTNESS TEMPERATURE

3.1 Choice of scheme

A real-time scheme to evaluate the performance of the cloud/radiation parameterization in an operational NWP model should make direct use of the standard analysis and forecast archive data if it is to be efficient. Since the model forecasts and analyses are archived at specific times (11Z and 23Z for the Bureau's model) this restricts the type of satellite data which can be used to that which is available at those times. For convenience in navigation and maximum area coverage at the fixed analysis times geostationary satellite data were selected for the validation scheme; initially GMS with the addition of GOES and METEOSAT in September 1993. One cost of using geostationary satellites is that they have only a limited number of spectral bands which may restrict the amount of cloud information which can be obtained. In fact in order to ensure that extraneous diurnal effects were not introduced into the data the choice was restricted to the infrared (IR) channel at 11μm (at least for GMS). Thus the validation scheme is not sensitive to the shortwave optical properties of cloud but should still provide a good evaluation for the amount and geographical placement of cloud produced by the model, at least at low and middle latitudes.

The basic cloud validation method chosen was a model-to-satellite method (Morcrette 1991), in which the archived model thermodynamic and diagnosed cloud fields were used as input into a special IR window version of the Fels-Schwarzkopf longwave radiation code to produce brightness temperature fields directly comparable with those from the geostationary satellites. Apart from navigation the only processing required for the satellite data itself was to convert brightness values to brightness temperature and average it onto the model's physics grid. The R31 (R53) grid consists of 96 (162) equally spaced longitudes and 80 (134) latitudes with a spacing corresponding to a Gaussian integration grid. The validation regions for each satellite were chosen to avoid large viewing angles and the consequent problems with quantitative interpretation of IR satellite data near the edges of the image due to limb effects. These choices also ensured a large number of pixels in each model grid box. The areas limits are given in Table 1 and some statistics for the distribution of the number of pixels over the validation domains are given in Table 2.

3.2 Description of scheme

The GMS-4 satellite imagery is received in real-time by the Bureau of Meteorology, navigated, and stored in the McIDAS "area" format (Suomi et al 1983). The IR images are stored at the full resolution of approximately 5 km at the satellite subpoint. The pixel values are calibrated by the JMA so that the corresponding brightness temperatures can be found from a fixed lookup table. GOES and METEOSAT imagery in McIDAS "area" format is obtained in near real-time, in a reduced resolution form. Standard

	Latitude	Longitude
GMS	47.5S - 47.5N	90E - 170W
GOES	47.5S - 47.5N	160W - 60W
METEO	47.5S - 47.5N	50W - 50E

Table 1 The approximate geographical limits of the validation domains chosen for the 3 geostationary satellites.

	Average	Minimum	Maximum
GMS	2555 (880)	860 (215)	4120 (1465)
GOES	695 (235)	225 (50)	1105 (405)
METEO	800 (270)	270 (70)	1315 (475)

Table 2 Statistics for the number of pixels in each model grid box for the R31 (R53) resolution models for the three validation regions. Note that GOES and METEOSAT data are at a lower resolution than the GMS data.

McIDAS routines are used to convert pixel values to brightness temperatures and navigate the images. These McIDAS areas are processed to generate average brightness temperatures on the model grid in the following procedure. The image coordinates of the corners of the model gaussian physics grid are first obtained from the appropriate satellite navigation algorithm. Although the edges of the model grid boxes are curved in image coordinates, they are assumed to be straight lines for computational ease. (This typically misassigns a sector of pixels at most two or three deep at R31 resolution to a grid box adjacent to their correct one but as this is a small proportion of the pixels in a grid box, and as they tend to be of similar properties to the ones that belong there anyway, this misassignment produces negligible errors and is less significant for R53). Once the equations of the boundary lines are calculated, the satellite image is scanned a line at a time, and the correct grid box for each pixel found by determining when a pixel is in a different grid box to its neighbour. A histogram of brightness values is thus formed for each grid box in the validation region. The histograms are then used to calculate a range of statistics, including the grid box average brightness temperature (henceforth denoted Tave), which are then compared with the corresponding model derived fields, and archived for further analysis.

In normal operation the model doesn't need to produce the narrow band radiances used by satellite

sensors (particularly with response function folded in) and so for efficiency reasons it is necessary to derive such radiances offline using all the appropriate fields from a standard archive of the model's fields. The offline brightness temperature code uses the two IR window bands of the Fels-Schwarzkopf radiation code (Schwarzkopf and Fels 1991) which cover the spectral region 800-990cm^{-1} and includes absorption due to the water vapour continuum and some water vapour lines. The response function for the GMS-4 satellite sensor was digitised in steps of 10cm^{-1} over the range 805-985cm^{-1} and folded into the integration over the band which accounts for the spectral variation of the Planck function. The resulting window radiation code was checked against clear sky line-by-line single profile reference calculations, yielding errors of less than 1K in effective brightness temperature. The global modelled brightness temperatures (denoted TBRI) are generated twice a day after the operational forecast suite has finished and uses the archived model cloud amounts and heights, temperature, water vapour and surface pressure fields. The spectral response functions for GOES and METEOSAT were assumed to be the same as that for GMS to enable the same global model calculation to be used for all three satellites.

3.3 **Results for GMS**

The geographical distribution of the monthly average brightness temperature shown for September 1994 in figures 2 and 3 are representative of the results over the entire validation period. The broadscale patterns are in quite good agreement, although the model produces a more zonal field overall. Although the model does capture the ITCZ and SPCZ it does not have the range of cold temperatures shown in the satellite data. In fact there are no values of TBRI below 250K anywhere in the whole domain whereas Tave has an extended region below this (minimum 237K) in the ITCZ. This result is directly attributable to the 'thin cloud' approximation which does not allow model cloud to appear in levels above 200hPa. In the 'original' cloud model (see Fig.1) cloud was allowed at higher levels but was found to generate very cold brightness temperatures due to the blackbody cloud assumption. The accompanying cold areas in the model caused problems with the regional models using the global model for boundary conditions and was a major factor in the change to the 'thin cloud' model. Another feature of the model is that it doesn't produce any brightness temperatures above 300K, in contrast to the satellite data which shows a large warm patch over northern Australia. This suggests that the model overestimates low level cloudiness over the continent during the month.

To assess the impact of the unrealistic assumption of blackbody cirrus in the model on the validation scheme, an additional set of brightness temperatures (denoted TBPH) were also calculated offline using the same model input fields in conjunction with the temperature dependent cirrus emissivity

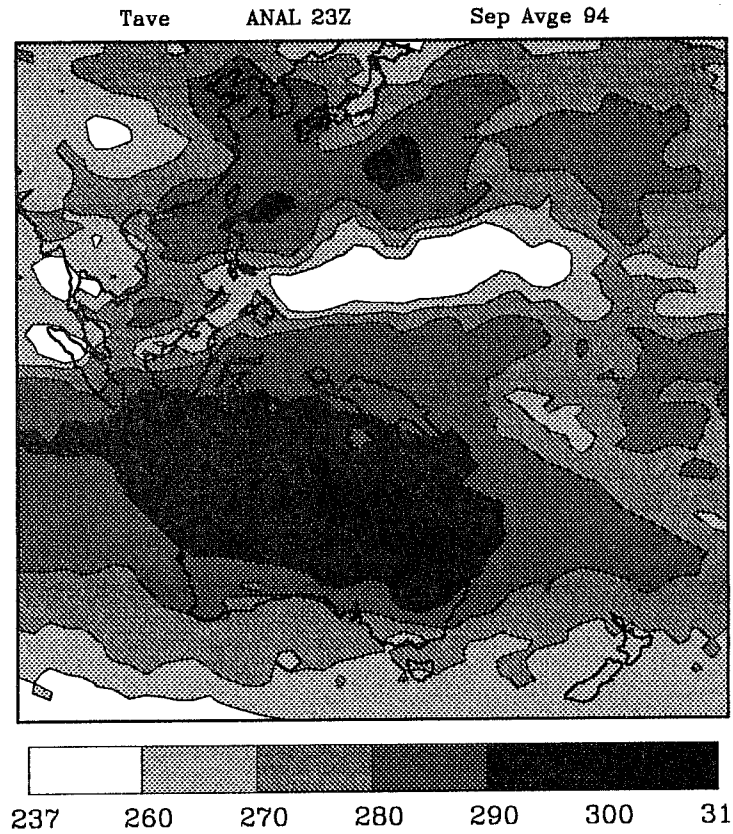

Figure 2 Monthly average brightness temperatures for September 1994 from GMS.

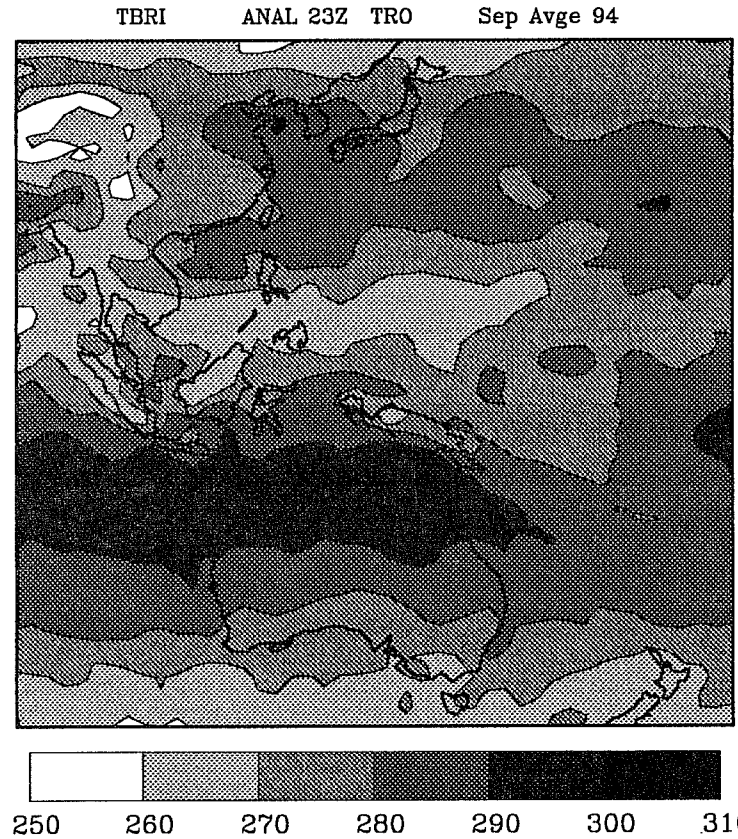

Figure 3 Monthly average of brightness temperature generated by the global model for September 1994.

parameterization of Platt and Harshvardhan (1988). Due to the restriction on high cloud temperatures provided by the 'thin cloud' model TBPH differs very little from TBRI, showing the same patterns but with the absence of some of the patches of cold temperature and with an approximately 1K warmer average over the GMS domain.

3.4 Results for GOES and METEOSAT

Figures 4 and 5 compare the satellite and model generated brightness temperatures for the GOES domain, again for the monthly average for September 1994. As for the GMS domain the model reproduces the broadscale pattern of the satellite data but is more zonal. The absence of cold model cloud over the tropical Pacific and South America is very pronounced and contributes substantially to the warm bias of about 4K in the area average over the entire domain when compared with the satellite data. There also seems to be a slight tendency for the model to produce too large an area of warm temperatures suggesting an underestimation of low level cloud frequencies or amounts.

The monthly averaged brightness temperatures for the METEOSAT region are shown in figures 6 and 7. In this case the tendency for zonality in the model is not obvious. The patterns over the land areas are in excellent agreement although there is a tendency for the model to overestimate the area of warm temperatures, particularly in the south and over the ocean. This is most likely due to the model underestimating the amounts of low cloud in these regions. The model has an area average bias of about 2K relative to the satellite.

4. VALIDATING CLOUD

4.1 The clear sky algorithm

Although brightness temperature provides an excellent field for model validation, because it is derived as a convolution over a number of model fields it can be difficult to determine which processes in the model simulation contribute to the errors. To aid in the diagnosis process the brightness temperature validation has been augmented by a simple scheme to derive cloud information from the satellite data that can be qualitatively compared with the cloud fields simulated by the model. This derivation of satellite cloud consists of two parts. The first uses a simple cloud identification scheme based on the infrared part of the ISCCP scheme (Rossow et al, 1985) to determine the clear sky fraction in each grid box, while the second is an attempt to stratify cloud into pseudo height classes. As noted above only the infrared image is used as the aim is to verify model cloud across the full diurnal cycle, while visible imagery is only available during daytime. Although the visible imagery could have been used when available, it was

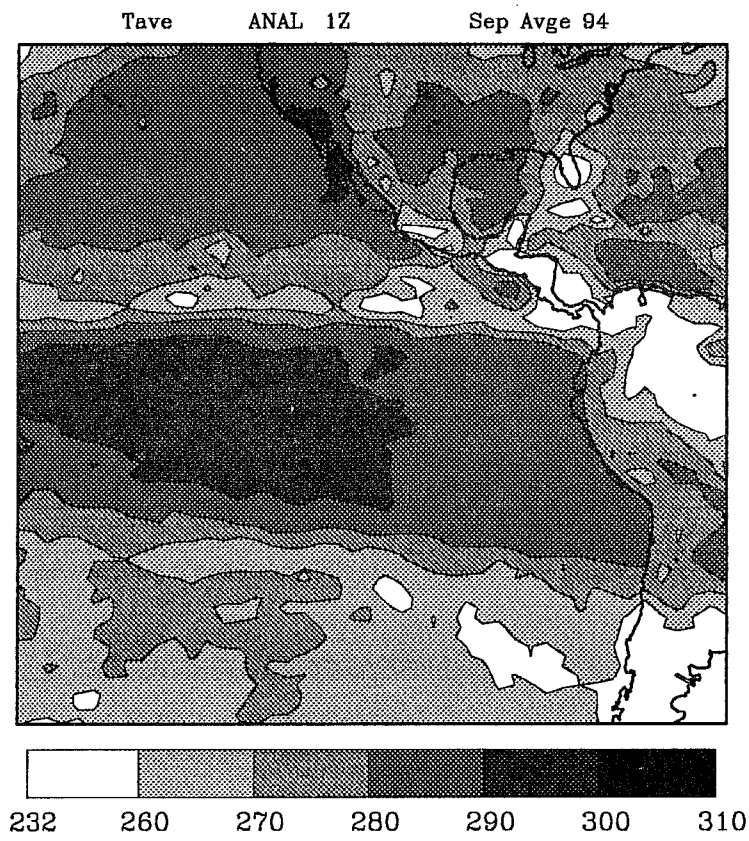

Figure 4 Monthly average brightness temperature from GOES for September 1994.

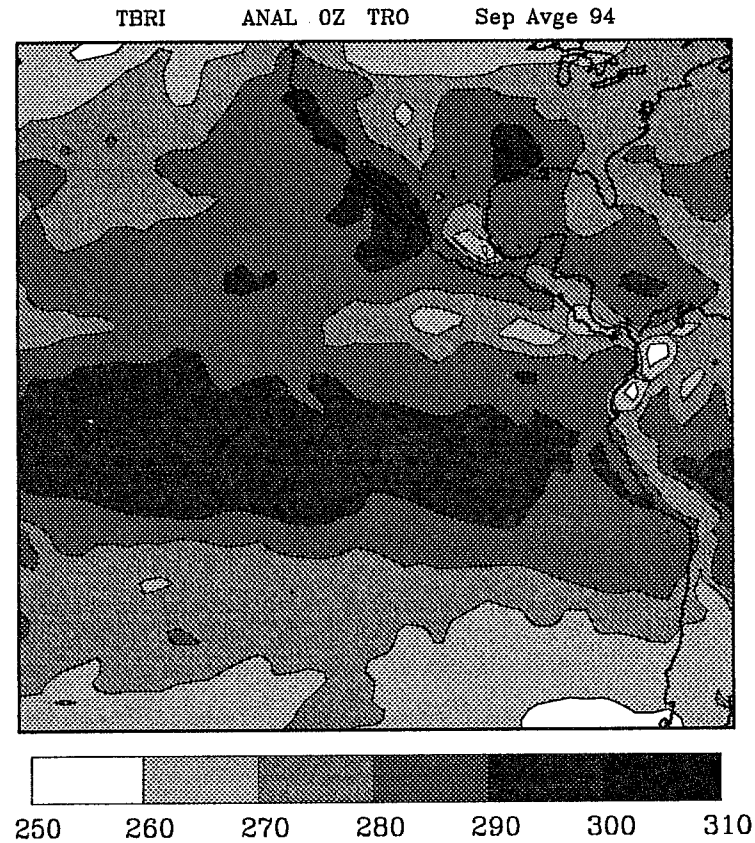

Figure 5 Monthly average of brightness temperature generated by the global model for September 1994 for the GOES domain.

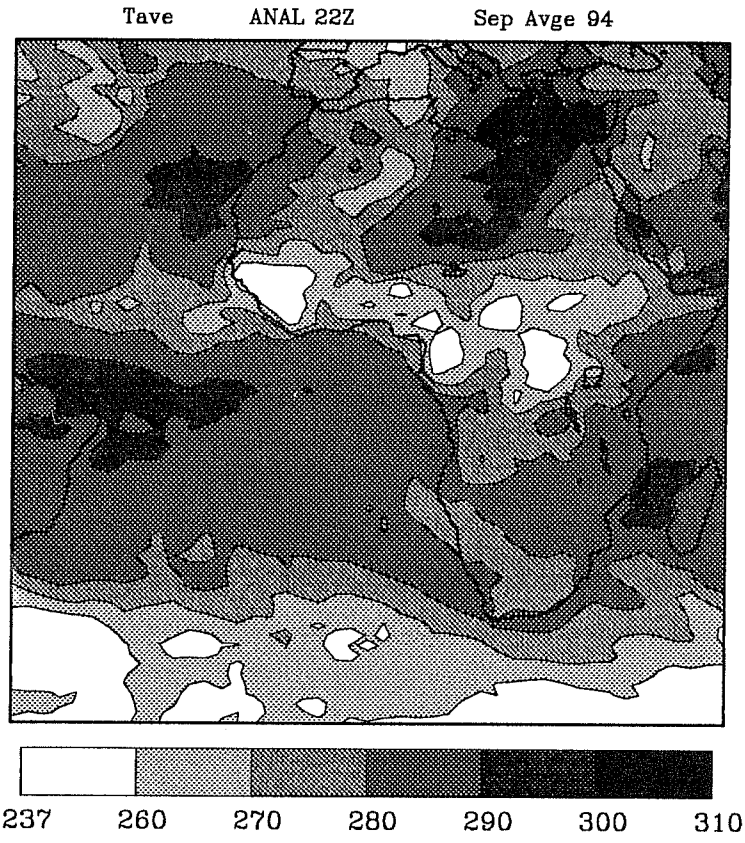

Figure 6 Monthly average brightness temperature from METEOSAT for September 1994.

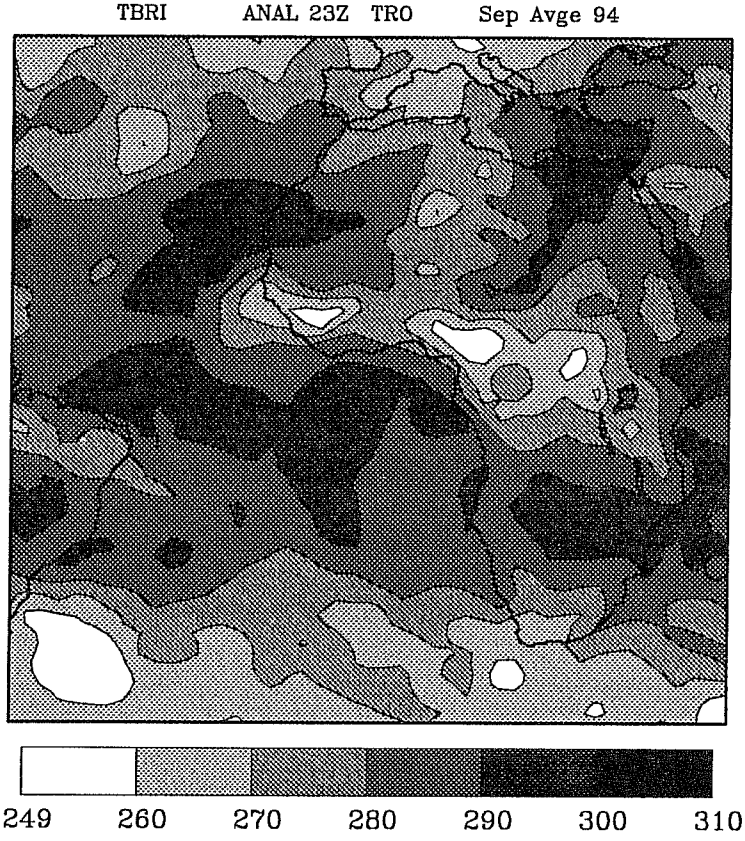

Figure 7 Monthly average of brightness temperature generated by the global model for September 1994 for the METEOSAT domain.

felt that to have done so would have inevitably skewed the results and unnecessarily complicated their interpretation.

The cloud clearing step follows the ISCCP philosophy of combining tests on spatial and temporal variability to determine whether a pixel is representative of "clear sky". In essence, the idea is that if a pixel is amongst the warmest within a certain radius of itself at the time of observation, and has a similar temperature on either the preceding or succeeding day, then it probably represents clear sky. The algorithm proceeds by first doing a spatial variability test. Each pixel's brightness temperature is compared with the maximum brightness temperature calculated over a 41 x 41 pixel square centred over it. If the pixel's own brightness temperature is more than 4 K cooler than this maximum, it is called "cloudy", otherwise "undecided". In the temporal variability test, if a pixel is more than 5 K cooler than the greater of the temperatures recorded 24 hours before or after, it passes the "cloudy test". If it is within 1.8 K of one of those temperatures, it passes the "clear test". (Note that it may pass both of these). The results of the spatial and temporal variability tests are then combined according to the table 3. Note that the comparison with images 24 hours either side of the actual observation automatically eliminates problems with the diurnal temperature range.

			Spatial test result	
			Cloudy	Undecided
Temporal variability tests	Cloudy	Clear	Mixed	Mixed
		Not clear	Cloudy	Cloudy
	Not cloudy	Clear	Mixed	Clear
		Not clear	Cloudy	Undecided

Table 3 Decision table showing how the results of the spatial variability test are combined with the results of the two temporal variability tests to determine which of the four categories (clear, cloudy, mixed and undecided) a pixel belongs to.

The various tolerances defined above, and the size of the box used for the spatial variability test, are all empirical constants. The values chosen are based on those used by ISCCP, and were verified by careful comparison with a subjective analysis of parts of several images, chosen to be representative of several meteorological regimes, including those for which "cloud clearing" is known to be difficult. One

difference is that the ISCCP algorithm uses different tolerances for land and sea based pixels. Given the coarse resolution of the model relative to the satellite, this was felt to be an unnecessary complication for our purposes, especially as the above was found to function adequately. The array of pixel types is used to produce additional diagnostic aids, including the clear sky brightness temperature mean and variance, and clear sky fraction, for each model grid box, as well as corresponding zonally averaged statistics across the analysis domain.

4.2 Cloud height

In the cloud height step, the histogram of brightness temperatures for each grid box is used to estimate the amount of cloud of each type (i.e. ultralow, low, middle, high or ultrahigh)[1] as defined by the cloud height limits of the model. This is done by direct comparison of the brightness temperature histograms with the model temperatures corresponding to the cloud layer limits at each grid point. (These layer limits assume cloud to be contiguous in the vertical and separate the layers shown for the 'original' model in Fig. 1). This procedure assumes that the model is accurate, the clouds are in thermal equilibrium with their surroundings, and that they are radiating as black bodies. Leaving aside the first of these, the second is quite reasonable at the global modelling scale, while the third is manifestly untrue in the case of optically thin cirrus. The scheme ran into early problems due to the mismatch between the model surface temperatures (the monthly climatology scheme for SST's), which as a monthly mean was often several degrees different from the clear sky brightness temperature diagnosed above. This was overcome by replacing the model surface temperature with an average of the model and diagnosed clear sky brightness temperature, weighted by the diagnosed clear sky fraction, but only if the clear sky fraction was greater than 0.1, so that the estimated clear sky brightness temperature was based on a reasonable number of pixels. A more serious shortcoming was that the scheme proved to be incapable of distinguishing between middle cloud, and optically thin cirrus, even when a correction for the reduced emissivity of this latter cloud was applied.

4.3 Results

Fig. 8 shows a comparison of model clear sky[2] fraction with results from the cloud clearing algorithm and from an annual time average derived from the ISCCP 1983 to 1988 data. GMS1 (the lower curve)

---

[1] Ultralow cloud is cloud below the bottom of the low cloud layer. Ultrahigh is cloud above the top of the high cloud layer.

[2] Model cloud is randomly overlapped.

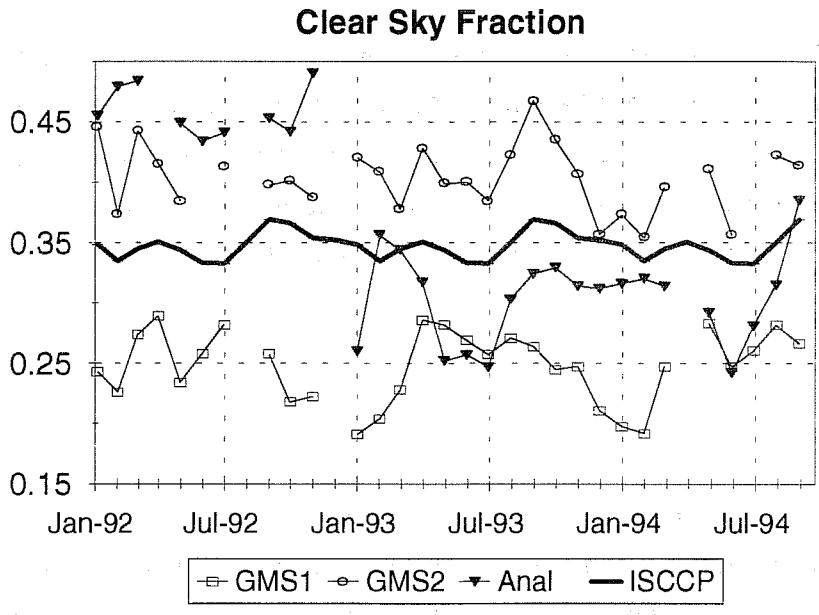

Figure 8 Time series of monthly clear sky fractions for the GMS domain. GMS1 is calculated from the 'clear' pixels, GMS2 from the sum of 'clear' and 'undecided' pixels.

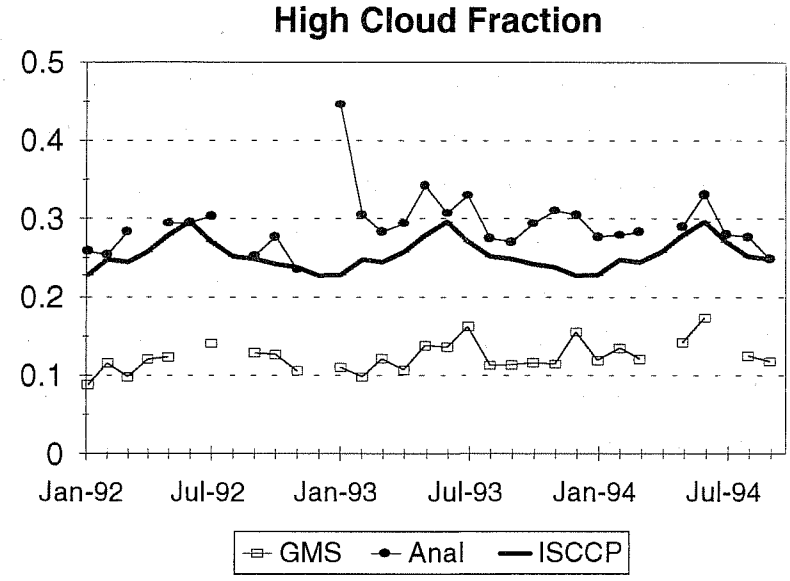

Figure 9 Time series of the monthly sums of high cloud fractions averaged over the GMS domain.

shows the fraction of unambiguously clear pixels in each grid box averaged over the GMS domain. GMS2 is the sum of clear and undecided pixels. These two estimates for clear sky fraction bracket the result derived from ISCCP for this region as expected. The model does not agree with the data, even in

the representation of seasonal trends. The R31L9 model clearly underestimated total cloud over the region. The change to 19 levels caused an overestimate of cloud cover which seems to have been initially corrected by the 'thin cloud' approximation in February 1993. After this the model shows a large increase of cloud cover which appears to be essentially a seasonal effect but may be enhanced by the change in the number of model levels. It is in disagreement with the GMS data which would suggest that the total cloud amount remains fairly constant from May to October. The model also misses the apparent decrease in clear sky fraction over the southern summer. The comparisons for high cloud in Fig. 9 show that the cloud height identification algorithm underestimates the high cloud amount substantially by comparison with ISCCP. Allowing for this bias, apart from the period around January 1993 the model does seem to follow the trends in the satellite data and is in reasonable agreement with the high cloud amounts derived from ISCCP. Fig. 10 shows a comparison of the cloud fraction due to the combination of high and middle cloud. Overall the model and GMS data appear to be in quite good agreement with each other as well as with the ISCCP results. The disagreements with clear sky fraction discussed above appear to be due to overestimation of low cloud. This was not obvious from the brightness temperatures in Fig. 2.

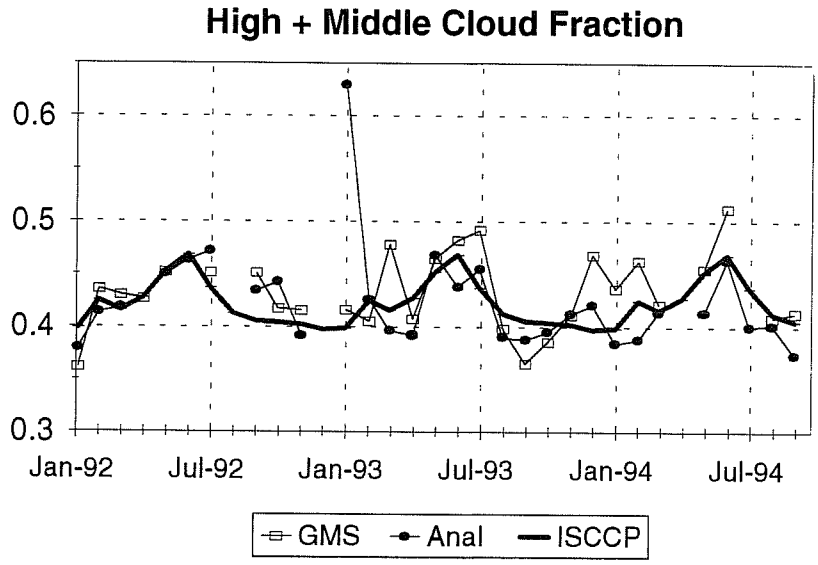

Figure 10 Time series of monthly averages for the sum of high and middle cloud for the GMS domain.

The results from the GOES and METEOSAT areas are similar but in both cases the model overestimate in the clear sky fraction relative to both ISCCP and the satellite data is larger. In contrast to the GMS case the high cloud amounts from the model are too large relative to ISCCP. The sum of high and

middle cloud for the model are almost identical to the ISCCP result for both domains. This implies that the model severely underestimates the low cloud amount over the GOES and METEOSAT domains. The differences in low cloud in the different regions is most likely the consequence of tuning the strato-cumulus cloud only to data from the GMS domain. When the number of levels in the model was increased the amount of low cloud increased substantially over time in some regions including the GMS domain but appears to have decreased in others.

6. FUTURE IMPROVEMENTS

There are a number of avenues for possible improvement in the validation scheme. The results from ISCCP and the availability of data from a number of geostationary satellites suggest that a simple global scheme could be implemented. The insensitivity of the 11μm brightness temperature to middle and low level cloud suggests a need for other spectral intervals to be considered and here the next series of geostationary satellites will provide a fairly wide choice. Currently there is the option of adding the visible channel (although this would be at the cost of restricting the validation to daytime) or the water vapour channel (6.3μm) but this is not yet available for GMS. The addition of the former would enable the full ISCCP cloud scheme to be implemented which would improve the height identification, as well as provide some validation for the model's shortwave cloud optical properties. It is not clear that the addition of the water vapour channel to the validation scheme would yield any more useful cloud information to that already available from the 11μm channel, given the current state of the cloud/radiation parameterization in the model.

Current plans are to incorporate higher resolution GOES and METEOSAT imagery, make the present scheme more robust and to test the utility of a pattern recognition algorithm (Ebert 1987) to better discriminate different cloud heights and regimes. The scheme will shortly be applied to the Bureau's Australian and tropical regional models. Ultimately improvement must come via improvements to model cloud parameterization including interactive cloud optical properties.

7. CONCLUSION

The BMRC cloud validation scheme allows constant validation of some aspects of the cloud/radiation interaction in the Australian Bureau of Meteorology's operational NWP models on a day to day basis. The comparison of model brightness temperatures with satellite IR data shows that the geographical distributions generated by the model are quite good. The area averaged amounts of model high and middle cloud are in good agreement with the satellite data partitioned into cloud amount and pseudo

height classes. Although the brightness temperatures are not very sensitive to low cloud, the combination of clear sky fraction and high and middle cloud amounts allow some inferences to be made about the low cloud in the model. The large differences in the behaviour of the diagnostic cloud scheme in the three different regions stresses the need for global satellite data. Tuning a parameterization for one region of the globe is not sufficient; global fields require global validation. Although the cloud validation scheme is simple it has been shown to be capable of providing useful and timely information about the medium range prediction model and will soon be applied to regional models.

References

Alexander, R.C., and R.L. Mobley, 1976: Monthly average sea-surface temperatures and ice-pack limits on a 1° global grid. *Mon. Wea. Rev.*, **104,** 143-148.

Anthes, R.A., 1977: A cumulus parameterization scheme utilizing a one-dimensional cloud model. *Mon. Wea. Rev.*, **105,** 270-286.

Cess, R.D., G.L. Potter, J.P. Blanchet, G.J. Boer, A.D. Del Genio, M. Déqué, V. Dymnikov, V. Galin, W.L. Gates, S.J. Ghan, J.T. Kiehl, A.A. Lacis, H. LeTreut, Z.-X. Li, X.-Z. Liang, B.J. McAvaney, V.P. Meleshko, J.F.B. Mitchell, J.-J. Morcrette, D.A. Randall, L. Rikus, E. Roeckner, J.F. Royer, U. Schlese, D.A. Sheinen, A. Slingo, K.E. Sokolov, K.E. Taylor, W.M. Washington, R.T. Wetherald, I. Yagai, and M.-H. Zhang, 1990: Intercomparison and interpretation of climate feedback processes in seventeen atmospheric general circulation models. *J. Geophys. Res.,95, 16601-16615.*

Ebert, E.E., 1987: A pattern recognition algorithm for distinguishing surface and cloud types in the polar regions. *J. Climate Appl. Meteor.*, **26,** 1412-1427.

Fels, S.B. and M.D. Schwarzkopf, 1975: The simplified exchange approximation: a new method for radiative transfer calculations. *J. Atmos. Sci.*, **32,** 1475.

Geleyn, J.-F. 1981: Some diagnostics of the cloud-radiation interaction in the ECMWF forecasting model. Workshop on Radiation and Cloud-Radiation Interaction in Numerical Modelling, 15-17 October 1980, ECMWF

Hart, T.L., W. Bourke, B.J. McAvaney, B.W.Forgan and J.L. McGregor, 1990: Atmospheric general circulation simulations with the BMRC global spectral model: the impact of revised physical parameterizations. *J. Climate,* **3,** 436-459.

Kuo, H.L., 1974: Further studies of the parameterization of the influence of cumulus convection on large-scale flow. *J. Atmos. Sci.*, **31,** 1232-1240.

Lacis, A.A., and J.E. Hansen, 1974: A parameterization for the absorption of solar radiation in the Earth's atmosphere. *J. Atmos. Sci.,***31,** 118-133.

Mitchell, K.E. and D.C. Hahn, 1990: Objective development of diagnostic cloud forecast schemes in global and regional models. *7th AMS Conference on Atmospheric Radiation,* San Francisco CA, J138-J145.

Morcrette, J.J 1991. Evaluation of model-generated cloudiness: satellite-observed and model-generated diurnal variability of brightness temperature. *Mon. Wea. Rev.,**119**, 1205-1224.*

Platt, C.M.R, and Harshvardhan 1988: Temperature dependence of cirrus extinction: implications for climate feedback. *J. Geophys. Res.*, **93**, 11051-11058.

Reynolds, R.W., and D.C. Marisco, 1993: An improved real-time global sea surface temperature analysis. *J. Climate,* **6,** 768-774

Rikus, L. 1991. The role of clouds in global climate modelling. *BMRC Research Report No. 25.*

Rikus, L. and J. Kepert, 1995: Validating cloud in a global operational NWP model. In preparation.

Rikus, L.J. and T. Hart, 1988: The development and refinement of a diagnostic cloud parameterization scheme for the BMRC global model, in *IRS '88: Current problems in atmospheric radiation*, ed. J. Lenoble and J-F. Geleyn

Rossow, W.B., F. Mosher, E. Kinsella, A. Arking, M. Desbois, E. Harrison, P. Minnis, E. Ruprecht, G. Seze, C. Simmer, and E. Smith, 1985: ISCCP cloud algorithm intercomparison. *J. Climate Appl. Meteor., **24**, 877-903.*

Rossow, W., and R.A. Schifer, 1991: ISCCP cloud data products. *Bull. Amer. Meteor. Soc.*, **72**, 2-20.

Schwarzkopf, M.D. and S.B. Fels, 1991: The simplified exchange method revisited: an accurate, rapid method for computation of infrared cooling rates and fluxes. *J. Geophys. Res., **96**, 9075-9096.*

Slingo, J.M. 1987. The development and verification of a cloud prediction scheme for the ECMWF model. *Q. J. R. Meteorol. Soc.*, **106**, 379-405.

Suomi, V.E., R. Fox, S.S. Limaye and W.L. Smith, 1983: McIDAS III: A modern interactive data access and analysis system. *J. Climat. Appl. Met.*, **22**, 766-78.

Tada, K.., W. Bourke, and T. Hart, 1989: An intercomparison of the numerical predictions of the BMRC and JMA global spectral models. *J. Meteor. Soc. Japan,* **67,** 705-729.